

Appearance of bulk superconductivity under hydrostatic pressure in Sr_{0.5}RE_{0.5}BiS₂ (RE=Ce, Nd, Pr, and Sm) compounds

Rajveer Jha, Brajesh Tiwari, and V. P. S. Awana

Citation: *Journal of Applied Physics* **117**, 013901 (2015); doi: 10.1063/1.4905391

View online: <http://dx.doi.org/10.1063/1.4905391>

View Table of Contents: <http://scitation.aip.org/content/aip/journal/jap/117/1?ver=pdfcov>

Published by the AIP Publishing

Articles you may be interested in

[Anomalous magnetism of Pr in PrCoAsO](#)

AIP Advances **4**, 017120 (2014); 10.1063/1.4862777

[Superconductivity at 5K in NdO_{0.5}F_{0.5}BiS₂](#)

J. Appl. Phys. **113**, 056102 (2013); 10.1063/1.4790322

[Bulk superconductivity at 5K in NdO_{0.5}F_{0.5}BiS₂](#)

AIP Conf. Proc. **1512**, 1106 (2013); 10.1063/1.4791433

[Complex magnetism and magneto-transport of RECoPO \(RE=La, Nd, and Sm\)](#)

J. Appl. Phys. **110**, 103913 (2011); 10.1063/1.3662151

[Control of magnetic ordering by altering Co–Co distances in La_{0.9}R_{0.1}Co₂P₂ \(R = Ce, Pr, Nd, and Sm\) phases with ThCr₂Si₂-type structures](#)

J. Appl. Phys. **107**, 09E316 (2010); 10.1063/1.3360186

The logo for AIP APL Photonics features the letters 'AIP' in a large, white, sans-serif font on the left, followed by a vertical orange bar and the words 'APL Photonics' in a smaller, white, sans-serif font on the right. The background is a dark red with a bright yellow sunburst effect in the center.

APL Photonics is pleased to announce
Benjamin Eggleton as its Editor-in-Chief



Appearance of bulk superconductivity under hydrostatic pressure in $\text{Sr}_{0.5}\text{RE}_{0.5}\text{FBiS}_2$ (RE = Ce, Nd, Pr, and Sm) compounds

Rajveer Jha, Brajesh Tiwari, and V. P. S. Awana^{a)}

CSIR-National Physical Laboratory, Dr. K.S. Krishnan Marg, New Delhi 110012, India

(Received 3 October 2014; accepted 20 December 2014; published online 5 January 2015)

We report the appearance of superconductivity under hydrostatic pressure (0–2.5 GPa) in $\text{Sr}_{0.5}\text{RE}_{0.5}\text{FBiS}_2$ with RE = Ce, Nd, Pr, and Sm. The studied compounds, being synthesized by solid state reaction route, are crystallized in tetragonal $P4/nmm$ space group. At ambient pressure, though the RE = Ce exhibits the onset of superconductivity below 2.7 K, the Nd, Pr, and Sm samples are not superconducting down to 2 K. With application of hydrostatic pressure (up to 2.5 GPa), superconducting transition temperature (T_c) is increased to around 10 K for all the studied samples. The magneto-resistivity measurements are carried out on all the samples under 2.5 GPa pressure and their upper critical fields (H_{c2}) are determined. The superconductivity of these compounds appears to be quite robust against magnetic field. Summarily, the $\text{Sr}_{0.5}\text{RE}_{0.5}\text{FBiS}_2$ compounds with RE = Ce, Nd, Pr, and Sm are successfully synthesized and superconductivity is induced in them under hydrostatic pressure. © 2015 AIP Publishing LLC.

[<http://dx.doi.org/10.1063/1.4905391>]

INTRODUCTION

BiS_2 based superconductivity was first observed at around 4.5 K in BiS_2 layers of $\text{Bi}_4\text{O}_4\text{S}_3$ compound.^{1,2} Later the same was seen in REO/FBiS_2 ^{3–12} compounds. In short span of time, the BiS_2 based superconductivity attracted tremendous interest from the scientific community.^{1–12} The principal reason for the same is that the layered structure of these compounds is exactly similar to that of famous $\text{REO}_{1-x}\text{F}_x\text{FeAs}$ pnictide high T_c superconductors. In case of $\text{REO}_{1-x}\text{F}_x\text{BiS}_2$, the charge carriers are introduced by O^{2-} site F^{1-} substitution in REO redox layer and superconductivity is established in adjacent BiS_2 layer. This is exactly same as being done in case of $\text{REO}_{1-x}\text{F}_x\text{FeAs}$, where O/F substitution in REO redox layer introduces superconductivity in adjacent FeAs.¹³ It is also reported that the superconductivity of BiS_2 based $\text{REO}_{1-x}\text{F}_x\text{BiS}_2$ compounds enhances tremendously under hydrostatic pressure.^{14–17} The increase in superconducting transition temperature (T_c) has been reported even up to five folds or so. For example, the T_c of $\text{LaO}_{0.5}\text{F}_{0.5}\text{BiS}_2$ increases from around 2.1 K to above 10 K under hydrostatic pressure of say, above 2 GPa.^{14,18} Researchers also synthesized the high pressure high temperature (HPHT) processed compounds of $\text{REO}_{1-x}\text{F}_x\text{BiS}_2$ series and established stable superconductivity of up to 10 K.¹⁶ As far as theoretical aspects are concerned, detailed electronic structure calculations are done and the role of sp orbitals of Bi and S is highlighted.^{19–21} The situation seems to be in parallel with Fe and As hybridization in case of Fe pnictide ($\text{REO}_{1-x}\text{F}_x\text{FeAs}$) superconductors.¹³ No doubt, the BiS_2 based recent superconductivity is catching the attention of scientific community.^{1–12,14–22}

It is proposed earlier that SrFBiS_2 is iso-structural to LaOBiS_2 , which may become superconducting with suitable doping.²³ In SrFBiS_2 , the carriers are introduced by Sr^{2+} site La^{3+} substitution, and superconductivity is achieved of up to 2.5 K.^{24–26} Also, the evolution of superconductivity is reported by substitution of tetravalent Th^{+4} , Hf^{+4} , Zr^{+4} , and Ti^{+4} for trivalent La^{+3} in LaOBiS_2 compound.²⁷ Interestingly, though in case of $\text{REO}_{1-x}\text{F}_x\text{BiS}_2$ superconductivity is reported for RE = La, Pr, Nd, and Ce,^{3–12} in SrFBiS_2 series only $\text{Sr}_{1-x}\text{La}_x\text{BiS}_2$ is yet studied.^{24–26} It was thus required to check upon the SrFBiS_2 series with Sr site different RE substitutions. Recently, we found that superconducting transition temperature (T_c) of $\text{Sr}_{0.5}\text{La}_{0.5}\text{FBiS}_2$ compound increases by five-fold from around 2 K to above 10 K, accompanied with a semiconducting to metallic transformation in normal state under just above 1 GPa external pressure.²⁸ Keeping all this in mind, in current article, we report successful synthesis of $\text{Sr}_{0.5}\text{RE}_{0.5}\text{FBiS}_2$ with RE = Ce, Nd, Pr, and Sm, and study their superconducting properties with and without application of hydrostatic pressure. It is found that though RE = Nd, Pr, and Sm do not show superconductivity down to 2 K, the RE = Ce exhibits the onset of superconductivity below 2.5 K. Interestingly, all the studied compounds demonstrated superconductivity of up to 10 K under hydrostatic pressure. Their magneto-transport measurements showed that these are quite robust against magnetic field. Here, we report on the synthesis and appearance of bulk superconductivity in $\text{Sr}_{0.5}\text{RE}_{0.5}\text{FBiS}_2$ systems with different RE (RE = Ce, Nd, Pr, and Sm) other than La.

EXPERIMENTAL DETAILS

The bulk polycrystalline samples of series $\text{Sr}_{0.5}\text{RE}_{0.5}\text{FBiS}_2$ (RE = Ce, Nd, Pr, and Sm) were synthesized by solid state reaction route via vacuum encapsulation. High purity Ce, Nd, Pr, Sm, SrF_2 , Bi, and S were weighed in

^{a)} Author to whom correspondence should be addressed. Electronic mail: awana@mail.nplindia.org. Tel.: +91-11-45609357. Fax: +91-11-45609310. URL: awanavps.wenbs.com

stoichiometric ratio and ground in pure Argon atmosphere filled glove box. The mixed powders were subsequently palletized and vacuum-sealed (10^{-4} mbar) in quartz tubes. The box furnace was used to sinter the samples at 650°C for 12 h with the typical heating rate of $2^\circ\text{C}/\text{min}$. The sintered samples were subsequently cooled down slowly to room temperature. This process was repeated twice. X-ray diffraction (XRD) patterns were recorded for all samples at room temperature in the scattering angular (2θ) range of 10° – 80° in equal 2θ step of 0.02° using *Rigaku Diffractometer* with CuK_α ($\lambda = 1.54 \text{ \AA}$) radiation. Rietveld analysis was performed for all samples using the standard *FullProf* program.

The pressure dependent resistivity measurements were performed on Physical Property Measurements System (PPMS-14 T, *Quantum Design*) using HPC-33 Piston type pressure cell with *Quantum design DC* resistivity Option. Hydrostatic pressures were generated by a BeCu/NiCrAl clamped piston-cylinder cell. The sample was immersed in a pressure transmitting medium (Daphne Oil) covered with a Teflon cell. Annealed Pt wires were affixed to gold-sputtered contact surfaces on each sample with silver epoxy in a standard four-wire configuration.

RESULTS

The room temperature observed and Rietveld fitted XRD patterns for the $\text{Sr}_{0.5}\text{RE}_{0.5}\text{FBiS}_2$ (RE = Ce, Nd, Pr, and Sm) compounds are shown in Figure 1. All the compounds are crystallized in tetragonal structure with space group $P4/nmm$. Small impurity peak of Bi_2S_3 is also observed in $\text{Sr}_{0.5}\text{Sm}_{0.5}\text{FBiS}_2$ compound, which is close to the background of XRD pattern. On the other hand, all the other studied samples are mostly phase pure within the XRD limit. Rietveld fitted lattice parameters are $a = 4.065(1)\text{ \AA}$, $c = 13.35(2)\text{ \AA}$ for $\text{Sr}_{0.5}\text{Ce}_{0.5}\text{FBiS}_2$; $a = 4.056(3)\text{ \AA}$, $c = 13.38(2)\text{ \AA}$ for $\text{Sr}_{0.5}\text{Nd}_{0.5}\text{FBiS}_2$; $a = 4.061(2)\text{ \AA}$, $c = 13.36(1)\text{ \AA}$ for $\text{Sr}_{0.5}\text{Pr}_{0.5}\text{FBiS}_2$, and $a = 4.053(1)\text{ \AA}$, $c = 13.40(2)\text{ \AA}$ for $\text{Sr}_{0.5}\text{Sm}_{0.5}\text{FBiS}_2$ compounds. It is worth mentioning that for the Sm-based compound, the intensity (profile) of peak around 26.5° , i.e.,

reflection (004) does not fit along with some other reflections like (005) and (007). These observations indicate a preferred orientation along c -crystallographic axis and/or impact of Sm atomic form factor, which may not be true for other RE compounds. We stick to the nominal composition for the refinement as changing the occupancy did not improve the fitting. The volume of the unit cell obtained through the Rietveld fitting analysis of each compound and other parameters, including their atomic co-ordinate positions, etc., are summarized in Table I. The volume of unit cell is increasing with the increasing ionic radii of the RE element from Sm to Ce. There is a possibility of internal chemical pressure on the unit cell of $\text{Sr}_{0.5}\text{RE}_{0.5}\text{FBiS}_2$, similar to that as in the case of $\text{REO}_{0.5}\text{F}_{0.5}\text{BiS}_2$ ^{3,5,10} with different RE.

The temperature dependent electrical resistivity $\rho(T)$ for the $\text{Sr}_{0.5}\text{RE}_{0.5}\text{FBiS}_2$ (RE = Ce, Nd, Pr, and Sm) compounds in the temperature range 2–300 K is shown in Figure 2. All the compounds show semiconducting behavior down to 2 K, except the $\text{Sr}_{0.5}\text{Ce}_{0.5}\text{FBiS}_2$, which exhibits the superconducting transition (T_c^{onset}) near 2.7 K, while $\rho = 0$ is not attained down to 2 K, see Figure 2. It is expected that the superconducting transition temperature (T_c) may increase with replacing La to Nd, Ce, Pr, and Sm, as in the case of $\text{REO}_{0.5}\text{F}_{0.5}\text{BiS}_2$ ^{3,10}. The T_c^{onset} is absent down to 2 K in these compounds, except for RE = Ce, which exhibits T_c^{onset} near 2.7 K. Interestingly, superconducting transition temperature (T_c) for similar structure Fe pnictides $\text{REFeAsO}/\text{F}$ ^{13,29} and BiS_2 based REO/FBiS_2 systems^{3–5,8–10} scales from around 26 K for La to 55 K for Sm in former (Fe-pnictides) and 2.1 K (La) to above 5 K (Nd) in later (BiS_2 based ones). The obvious RE ionic size dependence of T_c is not visible in currently studied $\text{Sr}_{0.5}\text{RE}_{0.5}\text{FBiS}_2$ system, and the reason behind the same is not clear. Seemingly, the chemical pressure on the unit cell is not large enough to bring in superconductivity in these compounds at ambient pressure. This is the reason that we applied external pressure on the studied $\text{Sr}_{0.5}\text{RE}_{0.5}\text{FBiS}_2$ compounds and achieved superconductivity in them, which will be discussed in Figures 4(a)–4(d).

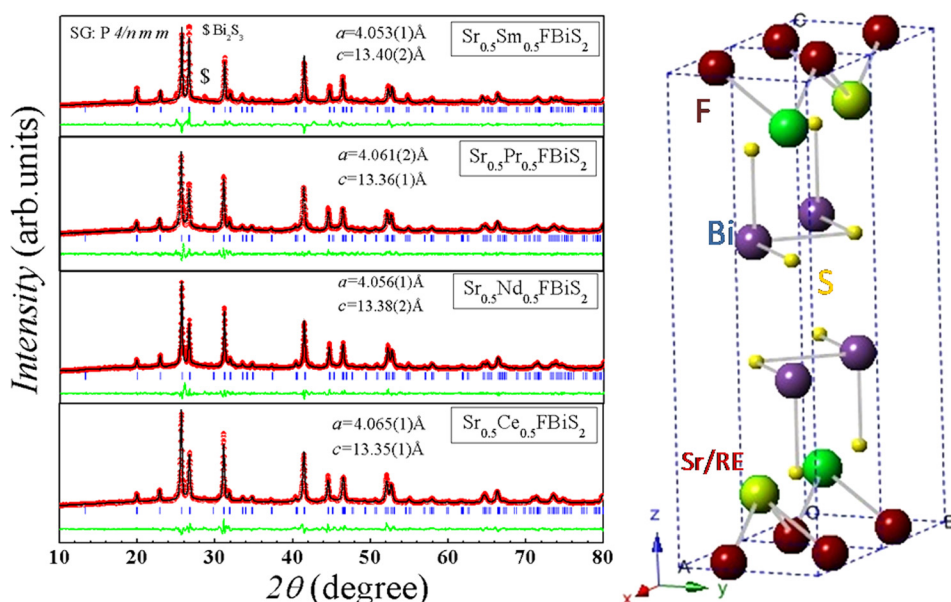


FIG. 1. Observed (open circles) and calculated (solid lines) XRD patterns of $\text{Sr}_{0.5}\text{RE}_{0.5}\text{FBiS}_2$ (RE = Ce, Nd, Pr, and Sm) compound at room temperature.

TABLE I. Atomic coordinates volume of unit cell, and Wyckoff positions, for studied $\text{Sr}_{0.5}\text{RE}_{0.5}\text{FBiS}_2$ compounds.

Samples	$\text{Sr}_{0.5}\text{Ce}_{0.5}\text{FBiS}_2$	$\text{Sr}_{0.5}\text{Nd}_{0.5}\text{FBiS}_2$	$\text{Sr}_{0.5}\text{Pr}_{0.5}\text{FBiS}_2$	$\text{Sr}_{0.5}\text{Sm}_{0.5}\text{FBiS}_2$
χ^2	4.19	3.54	4.58	6.33
Bragg R -factor	4.96	2.64	3.68	6.20
R_f -factor	3.52	1.82	3.43	4.68
$a=b(\text{\AA})$	4.065(1)	4.056(3)	4.061(2)	4.053(1)
$c(\text{\AA})$	13.35(2)	13.38(2)	13.36(1)	13.40(3)
c/a	3.28	3.29	3.28	3.30
$V(\text{\AA}^3)$	221.11(2)	220.22(3)	220.52(1)	220.35(3)
Sr/RE(1/4, 1/4, z)	0.110(1)	0.109(2)	0.114(1)	0.113(1)
Bi(1/4, 1/4, z)	0.623(3)	0.624(2)	0.624(3)	0.626(1)
S1(1/4, 1/4, z)	0.379(1)	0.381(1)	0.364(2)	0.363(3)
S2(1/4, 1/4, z)	0.809(2)	0.812(3)	0.810(1)	0.822(1)
F(x, y, z)	(3/4, 1/4, 0)	(3/4, 1/4, 0)	(3/4, 1/4, 0)	(3/4, 1/4, 0)

Figures 3(a)–3(d) depict the temperature dependence of DC magnetic susceptibility (field cool) from 300 K down to 2 K in applied field of 1 kOe for $\text{Sr}_{0.5}\text{RE}_{0.5}\text{FBiS}_2$ (RE = Ce, Nd, Pr, and Sm). Curie-Weiss law, $\chi = C/(T-\Theta)$, fitting was performed to determine the paramagnetic effective magnetic moments (μ_{eff}) and dominant magnetic ordering (sign of Θ). The estimated effective magnetic moments are $\mu_{\text{Ce}} = 2.97\mu_{\text{B}}/\text{f.u.}$ ($C = 1.19 \text{ emu.K/mol-Oe}$), $\mu_{\text{Nd}} = 2.87\mu_{\text{B}}/\text{f.u.}$ ($C = 1.429 \text{ emu.K/mol-Oe}$), $\mu_{\text{Pr}} = 3.14\mu_{\text{B}}/\text{f.u.}$ ($C = 1.24 \text{ emu.K/mol-Oe}$), $\mu_{\text{Sm}} = 3.24\mu_{\text{B}}/\text{f.u.}$ ($C = 1.31 \text{ emu.K/mol-Oe}$) for $\text{Sr}_{0.5}\text{Ce}_{0.5}\text{FBiS}_2$, $\text{Sr}_{0.5}\text{Nd}_{0.5}\text{FBiS}_2$, $\text{Sr}_{0.5}\text{Pr}_{0.5}\text{FBiS}_2$, and $\text{Sr}_{0.5}\text{Sm}_{0.5}\text{FBiS}_2$, respectively, and their corresponding Curie-Weiss temperature (Θ) are -216.31 K , -72.61 K , -59.18 K , and -160.90 K . The negative Θ for all the compounds suggests that the predominant magnetic ordering is antiferromagnetic. A clear magnetic transition can be seen in the upper inset of Figures 3(a) and 3(d) for $\text{Sr}_{0.5}\text{Ce}_{0.5}\text{FBiS}_2$ and $\text{Sr}_{0.5}\text{Sm}_{0.5}\text{FBiS}_2$ at around 8 K, which does not saturates down to 2 K under 1 kOe. After this submission in a preprint³⁰ for $\text{Sr}_{0.5}\text{Ce}_{0.5}\text{FBiS}_2$, a similar transition is observed at around 8 K, which was claimed to be of ferromagnetic nature being coexisting with superconductivity. Since the obtained Curie-Weiss temperature is negative, the predominant ordering seems to be antiferromagnetic, which can

be further complimented with isothermal magnetization (M - H) curves at 2 K. The M - H plots are shown in the lower insets of Figures 3(a)–3(d), which do not indicate any sign of saturation up to 5 kOe, though small loop opening is seen for RE = Ce and Sm, suggesting the canting of magnetic moments in these samples. A clear paramagnetic behavior is observed for $\text{Sr}_{0.5}\text{Nd}_{0.5}\text{FBiS}_2$ and $\text{Sr}_{0.5}\text{Pr}_{0.5}\text{FBiS}_2$ from the magnetization curves at 2 K, as can be viewed in the insets of Figures 3(b) and 3(c), respectively.

Figures 4(a)–4(d) show temperature dependent electrical resistivity $\rho(T)$ at various applied pressures of 0–2.5 GPa in the temperature range 2–300 K for the $\text{Sr}_{0.5}\text{RE}_{0.5}\text{FBiS}_2$ (RE = Ce, Nd, Pr, and Sm) compounds. Though normal state resistivity shows the semiconducting behavior up to applied hydrostatic pressure of 1.5 GPa for all the samples, but the resistivity values are suppressed remarkably. Interestingly, the normal state resistivity changes from semiconducting to the metallic one at 2.0 and 2.5 GPa applied pressures for all the samples. Inset of Figures 4(a)–4(d), i.e., the magnified view of resistivity curves show clear superconducting transitions at various pressures. Apart from $\text{Sr}_{0.5}\text{Ce}_{0.5}\text{FBiS}_2$, the other compounds did not show superconducting onset at ambient pressure. Sufficient broadening in the superconducting transitions is observed under applied pressure of 1.5 GPa for $\text{Sr}_{0.5}\text{Ce}_{0.5}\text{FBiS}_2$, $\text{Sr}_{0.5}\text{Nd}_{0.5}\text{FBiS}_2$, and $\text{Sr}_{0.5}\text{Sm}_{0.5}\text{FBiS}_2$ and at 0.97 GPa for $\text{Sr}_{0.5}\text{Pr}_{0.5}\text{FBiS}_2$. Also the onset of superconducting transition (T_c^{onset}) increases with increasing pressure.

Figure 5 shows the pressure dependence of the superconducting transition temperature (T_c^{onset}) for the studied $\text{Sr}_{0.5}\text{RE}_{0.5}\text{FBiS}_2$ (RE = Ce, Nd, Pr, and Sm) compounds. It can be inferred that superconductivity gradually increases with pressure up to the 0.97 GPa for all the samples. For higher pressure of 1.5 GPa, the T_c^{onset} shoots up to above 9 K. It seems that 1.5 GPa is the transition pressure (P_t) for all the samples. With further increase in the pressure, though the T_c^{onset} gets almost saturated, the $T_c(\rho=0)$ is increased, resulting in relatively sharper superconducting transition widths in the pressure range of 1.5–2.5 GPa. In our results, we also observed slight decreases in T_c^{onset} for $\text{Sr}_{0.5}\text{Ce}_{0.5}\text{FBiS}_2$ and $\text{Sr}_{0.5}\text{Sm}_{0.5}\text{FBiS}_2$ samples at the 2.5 GPa pressure; otherwise the trend of enhancement of superconductivity under pressure is same for all the samples.

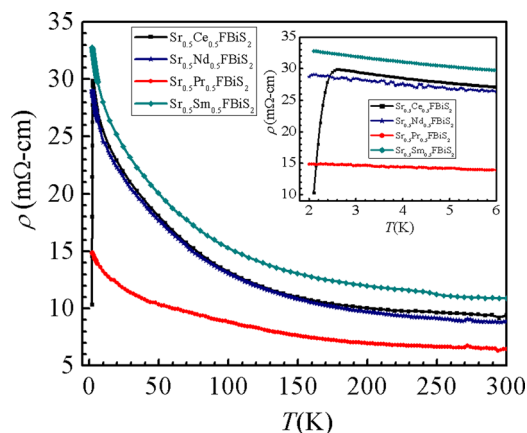


FIG. 2. Resistivity versus temperature $\rho(T)$ plots for $\text{Sr}_{0.5}\text{RE}_{0.5}\text{FBiS}_2$ compounds, at ambient pressure in the temperature range 300 K–2 K. Inset shows the $\rho(T)$ curve in the temperature range 6–2 K.

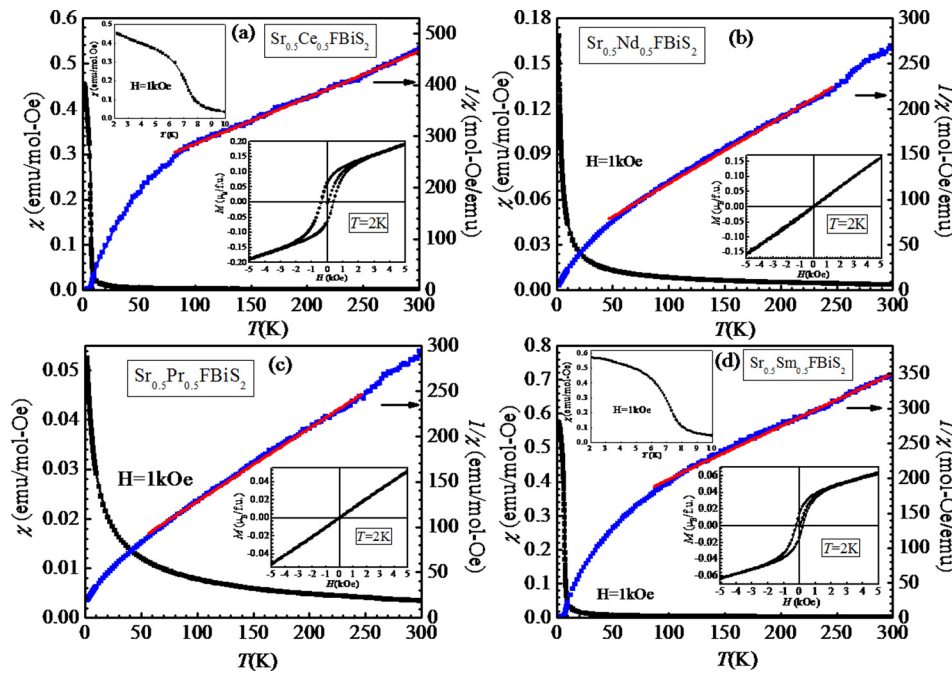


FIG. 3. (a)-(d) Temperature dependent magnetic susceptibility $\chi(T)$ for (a) $\text{Sr}_{0.5}\text{Ce}_{0.5}\text{FBiS}_2$, (b) $\text{Sr}_{0.5}\text{Nd}_{0.5}\text{FBiS}_2$, (c) $\text{Sr}_{0.5}\text{Pr}_{0.5}\text{FBiS}_2$, and (d) $\text{Sr}_{0.5}\text{Sm}_{0.5}\text{FBiS}_2$ compounds at ambient pressure. The upper inset of (a) and (d) is zoomed part in the temperature range 2–10 K and lower inset of each (a)-(d) shows the isothermal magnetization at 2 K.

Figures 6(a)–6(d) show the $\rho(T)$ under applied magnetic fields (1–7 T) for the $\text{Sr}_{0.5}\text{RE}_{0.5}\text{FBiS}_2$ (RE = Ce, Nd, Pr, and Sm) under applied pressure of 2.5 GPa. It is worth noting that with increasing magnetic field, the $T_c(\rho=0)$ decreases more rapidly as compared to the T_c^{onset} . In these compounds, the superconducting transition width is broadened under applied magnetic fields, which is similar to high- T_c cuprates and Fe-based pnictide superconductors. We summarize the magneto-resistivity results for all studied compounds as critical fields versus temperature phase diagrams, which is being shown in Figures 7(a)–7(d). The critical fields are estimated

at corresponding temperatures, where resistivity drops to 90%, 50%, and 10% of the normal state resistance [$\rho_n(T, H)$] in applied magnetic fields. The upper critical field, $H_{c2}(T)$ (using 90% criteria) at absolute zero temperature $H_{c2}(0)$ is determined by the conventional one-band Werthamer–Helfand–Hohenberg (WHH) equation, i.e., $H_{c2}(0) = -0.693T_c(dH_{c2}/dT)_{T=T_c}$. The estimated $H_{c2}(0)$ are 13.8 T, 11.6 T, 13.5 T, and 14.5 T for $\text{Sr}_{0.5}\text{Ce}_{0.5}\text{FBiS}_2$, $\text{Sr}_{0.5}\text{Nd}_{0.5}\text{FBiS}_2$, $\text{Sr}_{0.5}\text{Pr}_{0.5}\text{FBiS}_2$, and $\text{Sr}_{0.5}\text{Sm}_{0.5}\text{FBiS}_2$, respectively. In Figures 7(a)–7(d), the solid lines are the extrapolation to the Ginzburg–Landau equation $H_{c2}(T) = H_{c2}(0)(1-t^2/1+t^2)$,

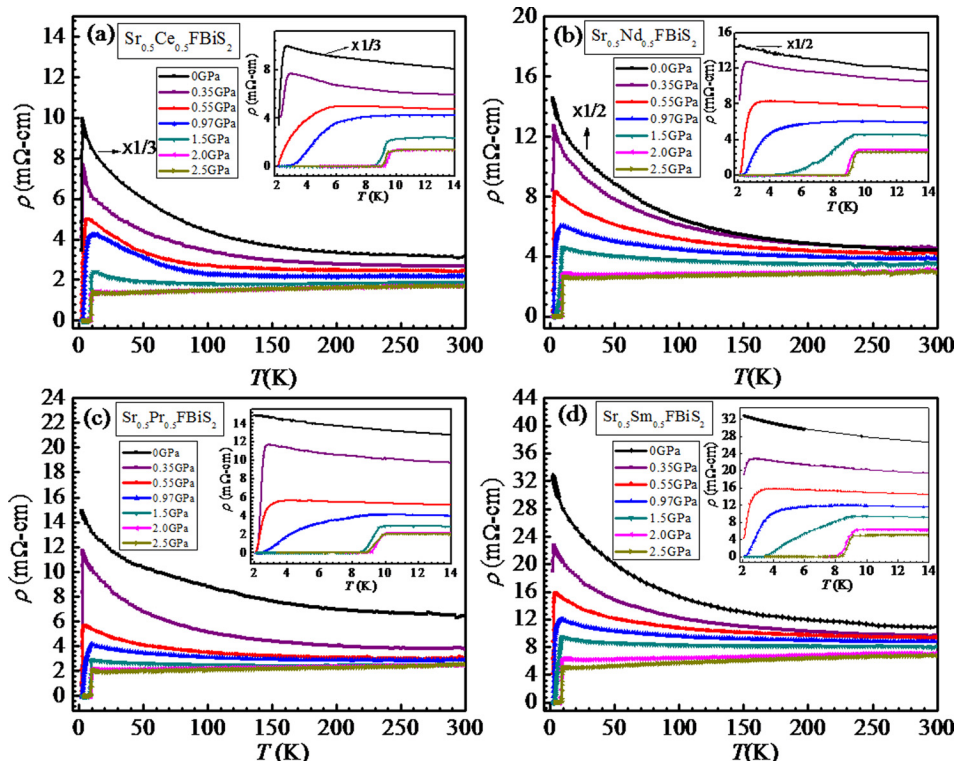


FIG. 4. (a)-(d) Resistivity versus temperature $\rho(T)$ plots at various applied pressures (0–2.5 GPa) in the temperature range 300 K–2.0 K, inset of each shows the zoomed part of $\rho(T)$ plots near the superconducting transition temperature for (a) $\text{Sr}_{0.5}\text{Ce}_{0.5}\text{FBiS}_2$, (b) $\text{Sr}_{0.5}\text{Nd}_{0.5}\text{FBiS}_2$, (c) $\text{Sr}_{0.5}\text{Pr}_{0.5}\text{FBiS}_2$, and (d) $\text{Sr}_{0.5}\text{Sm}_{0.5}\text{FBiS}_2$ compounds.

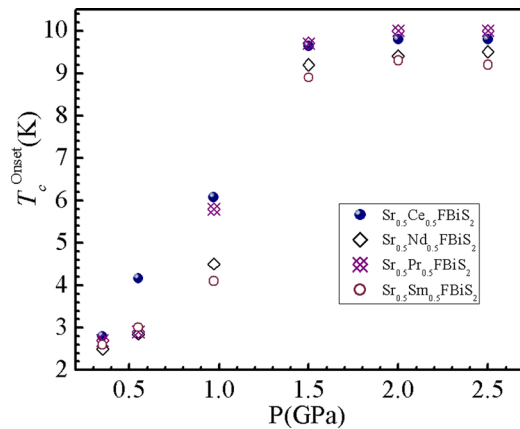


FIG. 5. T_c^{onset} vs applied pressure for the $\text{Sr}_{0.5}\text{RE}_{0.5}\text{FBiS}_2$ compounds.

where $t = T/T_c$ is the reduced temperature, which gives values slightly higher than that by *WHH* approach. These upper critical field values for all samples are close to but within the Pauli paramagnetic limit, i.e., $H_p = 1.84T_c$. The liquid vortex region between irreversible field $H_{\text{irr}}(T)$ and upper critical field $H_{c2}(T)$ is of significant importance for a superconductor. H_{irr} is determined using 10% criteria of magnetoresistivity and is slightly less than half of the upper critical field.

DISCUSSION

Rare-earth substituted BiS_2 -based layered compounds $\text{Sr}_{0.5}\text{RE}_{0.5}\text{FBiS}_2$ (RE = Ce, Nd, Pr, and Sm) are crystallized in tetragonal structure with space group $P4/nmm$. The choice of different RE-ions in these $\text{Sr}_{0.5}\text{RE}_{0.5}\text{FBiS}_2$ (RE = Ce, Nd, Pr, and Sm) compounds is based on the fact that superconductivity has yet been reported only for $\text{Sr}_{0.5}\text{La}_{0.5}\text{FBiS}_2$,^{24–26} which curiously increased from 2.5 K to 10 K under external

hydrostatic pressure.²⁸ It is important to note that there is nearly no effect of different RE-ions on the c lattice parameter however a decreases with the ionic radii of RE-ion in $\text{Sr}_{0.5}\text{RE}_{0.5}\text{FBiS}_2$. Under ambient pressure, the studied compounds show semiconductor like conduction in normal state with minimum resistivity for $\text{Sr}_{0.5}\text{Pr}_{0.5}\text{FBiS}_2$ at room temperature. Apart from $\text{Sr}_{0.5}\text{Ce}_{0.5}\text{FBiS}_2$, none of the other studied compounds showed onset of superconducting transition down to 2 K. Under hydrostatic pressure starting from 0.25 GPa to 2.50 GPa, all these compounds showed superconductivity with T_c^{onset} reaching up to 9–10 K. The sharp increase in T_c^{onset} under up to 1.5 GPa pressure and its further saturation for higher pressures suggest possible structural change in these Pauli paramagnetic limited ($H_p \sim 1.84T_c$) superconductors with applied hydrostatic pressure. Based on structural and magnetic studies, Tomita *et al.*³¹ have argued in similar BiS_2 -based compound ($\text{LaO}_{1-x}\text{F}_x\text{BiS}_2$) that a sudden increase of T_c with pressure is related to the structural transition from tetragonal to monoclinic. The significant increases in the T_c as well as the suppression of semiconducting behavior in the normal state resistivity suggest increase in the charge carrier density in the pressure range of 0–1.5 GPa. In similar structure, $\text{LnO}_{0.5}\text{F}_{0.5}\text{BiS}_2$ (Ln-La, Ce) compounds, Wolowiec *et al.*, have suggested the possibility of coexistence of two superconducting phases near 1.0 GPa pressure.¹⁶ In a study on single crystal of $\text{PrO}_{0.5}\text{F}_{0.5}\text{BiS}_2$, the normal state resistivity changed from semiconducting-like behavior to metallic behavior under pressure and T_c increased from 3.5 K to 8.5 K.³² A recently appeared preprint based on detailed first principle calculations by Morice *et al.*, for a similar set of compounds, i.e., $\text{LnO}_{1-x}\text{F}_x\text{BiS}_2$ (Ln = La, Ce, Pr, and Nd), especially the CeOBiS_2 concluded that these compounds

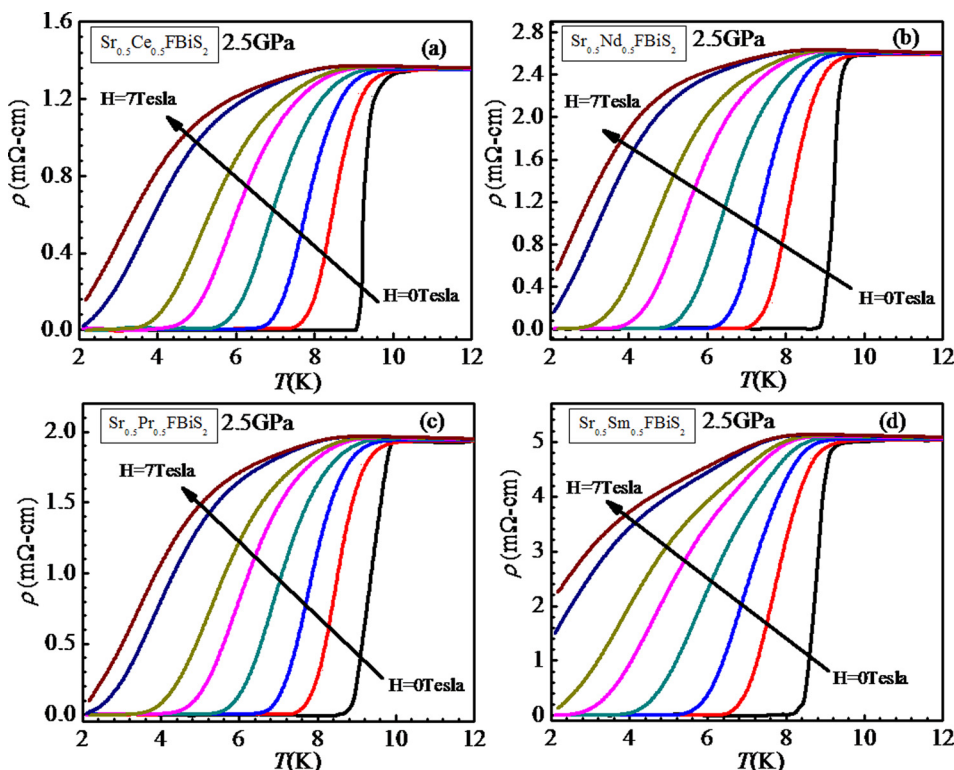


FIG. 6. (a)–(d) Temperature dependence of the Resistivity $\rho(T)$ under magnetic fields at 2.5 GPa hydrostatic pressure for (a) $\text{Sr}_{0.5}\text{Ce}_{0.5}\text{FBiS}_2$, (b) $\text{Sr}_{0.5}\text{Nd}_{0.5}\text{FBiS}_2$, (c) $\text{Sr}_{0.5}\text{Pr}_{0.5}\text{FBiS}_2$, and (d) $\text{Sr}_{0.5}\text{Sm}_{0.5}\text{FBiS}_2$ compounds.

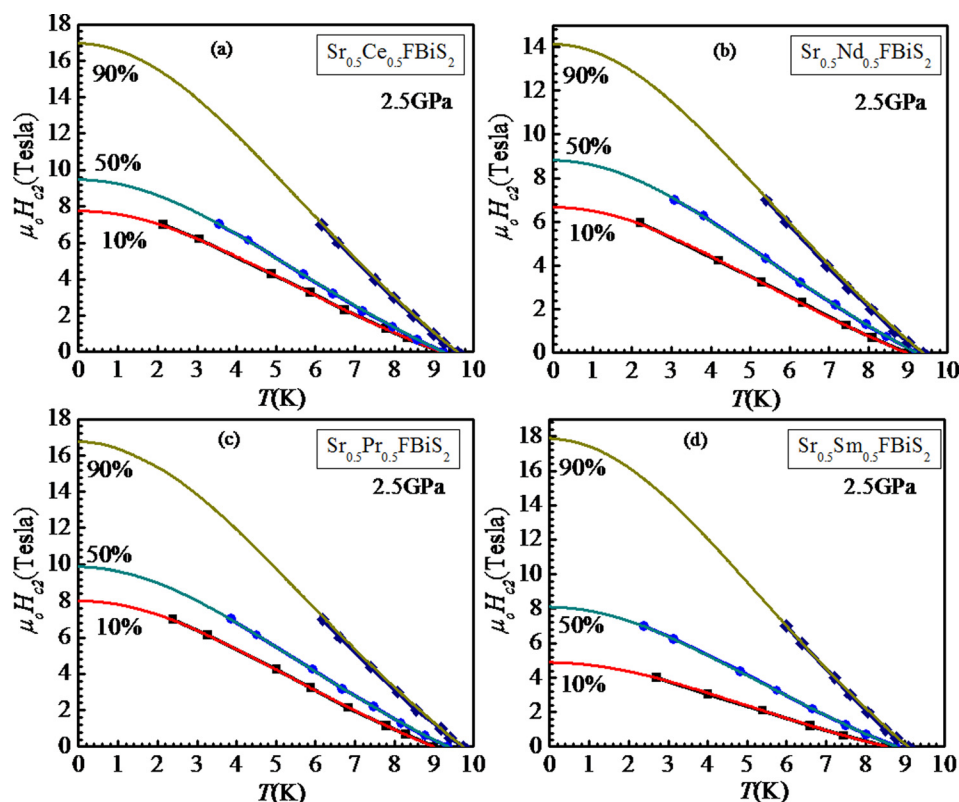


FIG. 7. (a)-(d) The temperature dependence of upper critical field H_{c2} and H_{irr} , determined from 90% and 10% resistivity criterion, respectively, for (a) $\text{Sr}_{0.5}\text{Ce}_{0.5}\text{FBiS}_2$, (b) $\text{Sr}_{0.5}\text{Nd}_{0.5}\text{FBiS}_2$, (c) $\text{Sr}_{0.5}\text{Pr}_{0.5}\text{FBiS}_2$, and (d) $\text{Sr}_{0.5}\text{Sm}_{0.5}\text{FBiS}_2$ compounds.

may display a pressure induced semiconducting to metal transition and also the change of rare-earth does not affect the Fermi surface.³³ There is a possibility of enhancement of strong electron correlations as well within same crystallographic phase under pressure. The pressure dependent structural studies are warranted on presently studied $\text{Sr}_{0.5}\text{RE}_{0.5}\text{FBiS}_2$ (RE = Ce, Nd, Pr, and Sm) compounds. This could help in knowing the possible reason behind dramatic changes in their transport properties, including appearance of superconductivity and normal state semiconducting to metallic transformation under moderate pressure of around 1.5 GPa. The resistivity under magnetic field at the pressure of 2.5 GPa exhibited a gradual decrease in T_c with increasing magnetic field, suggesting that these compounds are type-II superconductors. The upper critical fields being determined by WHH model are close to but within the Pauli paramagnetic limit, i.e., $H_p = 1.84T_c$. Also the upper critical field is almost double to as compared to irreversibility field at absolute zero temperature. The verification of these observations for layered fluorosulfide $\text{Sr}_{0.5}\text{RE}_{0.5}\text{FBiS}_2$ (RE = Ce, Nd, Pr, and Sm) may need further magnetometry studies under hydrostatic pressure.

In summary, we have synthesized layered fluorosulfide compounds $\text{Sr}_{0.5}\text{RE}_{0.5}\text{FBiS}_2$ (RE = Ce, Nd, Pr, and Sm), which are crystallized in tetragonal $P4/nmm$ space group. These compounds are semiconducting in the temperature range 300–2 K at ambient pressure and become metallic under pressures above 1.5 GPa. All the compounds show superconductivity under hydrostatic pressure with T_c^{onset} of 10 K. In resistivity under magnetic field measurements at the applied pressure of 2.5 GPa, these compounds appear to be quite robust against magnetic field.

ACKNOWLEDGMENTS

Authors would like to thank their Director NPL India for his keen interest in the present work. This work was financially supported by *DAE-SRC* outstanding investigator award scheme on search for new superconductors. Rajveer Jha acknowledges the *CSIR* for the senior research fellowship.

- ¹Y. Mizuguchi, H. Fujihisa, Y. Gotoh, K. Suzuki, H. Usui, K. Kuroki, S. Demura, Y. Takano, H. Izawa, and O. Miura, *Phys. Rev. B* **86**, 220510(R) (2012).
- ²S. K. Singh, A. Kumar, B. Gahtori, G. Sharma, S. Patnaik, and V. P. S. Awana, *J. Am. Chem. Soc.* **134**, 16504 (2012).
- ³Y. Mizuguchi, S. Demura, K. Deguchi, Y. Takano, H. Fujihisa, Y. Gotoh, H. Izawa, and O. Miura, *J. Phys. Soc. Jpn.* **81**, 114725 (2012).
- ⁴J. Xing, S. Li, X. Ding, H. Yang, and H. H. Wen, *Phys. Rev. B* **86**, 214518 (2012).
- ⁵V. P. S. Awana, A. Kumar, R. Jha, S. K. Singh, A. Pal, Shrutii, J. Saha, and S. Patnaik, *Solid State Commun.* **157**, 21 (2013).
- ⁶D. Yazici, K. Huang, B. D. White, A. H. Chang, A. J. Friedman, and M. B. Maple, *Philos. Mag.* **93**, 673 (2013).
- ⁷K. Deguchi, Y. Mizuguchi, S. Demura, H. Hara, T. Watanabe, S. J. Denholme, M. Fujioka, H. Okazaki, T. Ozaki, H. Takeya, T. Yamaguchi, O. Miura, and Y. Takano, *Euro Phys. Lett.* **101**, 17004 (2013).
- ⁸R. Jha, A. Kumar, S. K. Singh, and V. P. S. Awana, *J. Supercond. Novel Magn.* **26**, 499 (2013).
- ⁹R. Jha, H. Kishan, and V. P. S. Awana, *J. Appl. Phys.* **115**, 013902 (2014).
- ¹⁰S. Demura, Y. Mizuguchi, K. Deguchi, H. Okazaki, H. Hara, T. Watanabe, S. J. Denholme, M. Fujioka, T. Ozaki, H. Fujihisa, Y. Gotoh, O. Miura, T. Yamaguchi, H. Takeya, and Y. Takano, *J. Phys. Soc. Jpn.* **82**, 033708 (2013).
- ¹¹R. Jha and V. P. S. Awana, *Mater. Res. Express* **1**, 016002 (2014).
- ¹²R. Jha, A. Kumar, S. K. Singh, and V. P. S. Awana, *J. Appl. Phys.* **113**, 056102 (2013).
- ¹³Y. Kamihara, T. Watanabe, M. Hirano, and H. Hosono, *J. Am. Chem. Soc.* **130**, 3296 (2008).

- ¹⁴H. Kotegawa, Y. Tomita, H. Tou, H. Izawa, Y. Mizuguchi, O. Miura, S. Demura, K. Deguchi, and Y. Takano, *J. Phys. Soc. Jpn.* **81**, 103702 (2012).
- ¹⁵G. K. Selvan, M. Kanagaraj, S. E. Muthu, R. Jha, V. P. S. Awana, and S. Arumugam, *Phys. Status Solidi RRL* **7**, 510 (2013).
- ¹⁶C. T. Wolowiec, D. Yazici, B. D. White, K. Huang, and M. B. Maple, *Phys. Rev. B* **88**, 064503 (2013).
- ¹⁷C. T. Wolowiec, B. D. White, I. Jeon, D. Yazici, K. Huang, and M. B. Maple, *J. Phys. Condens. Matter* **25**, 422201 (2013).
- ¹⁸R. Jha, H. Kishan, and V. P. S. Awana, *J. Phys. Chem. Solids* "Effect of Hydrostatic pressures on the superconductivity of new BiS₂ based REO_{0.5}F_{0.5}BiS₂ (RE-la, Pr and ND) superconductors" (to be published).
- ¹⁹H. Usui, K. Suzuki, and K. Kuroki, *Phys. Rev. B* **86**, 220501(R) (2012).
- ²⁰G. Martins, A. Moreo, and E. Dagotto, *Phys. Rev. B* **87**, 081102(R) (2013).
- ²¹X. Wan, H. C. Ding, S. Y. Savrasov, and C. G. Duan, *Phys. Rev. B* **87**, 115124 (2013).
- ²²T. Yildirim, *Phys. Rev. B* **87**, 020506(R) (2013).
- ²³H. Lei, K. Wang, M. Abeykoon, E. S. Bozin, and C. Petrovic, *Inorg. Chem.* **52**, 10685 (2013).
- ²⁴X. Lin, X. Ni, B. Chen, X. Xu, X. Yang, J. Dai, Y. Li, X. Yang, Y. Luo, Q. Tao, G. Cao, and Z. Xu, *Phys. Rev. B* **87**, 020504(R) (2013).
- ²⁵Y. Li, X. Lin, L. Li, N. Zhou, X. Xu, C. Cao, J. Dai, L. Zhang, Y. Luo, W. Jiao, Q. Tao, G. Cao, and Z. Xu, *Supercond. Sci. Technol.* **27**, 035009 (2014).
- ²⁶H. Sakai, D. Kotajima, K. Saito, H. Wadati, Y. Wakisaka, M. Mizumaki, K. Nitta, Y. Tokura, and S. Ishiwata, *J. Phys. Soc. Jpn.* **83**, 014709 (2014).
- ²⁷D. Yazici, K. Huang, B. D. White, I. Jeon, V. W. Burnett, A. J. Friedman, I. K. Lum, M. Nallaiyan, S. Spagna, and M. B. Maple, *Phys. Rev. B* **87**, 174512 (2013).
- ²⁸R. Jha, B. Tiwari, and V. P. S. Awana, *J. Phys. Soc. Jpn.* **83**, 063707 (2014).
- ²⁹L. Li, Y. Li, Y. Jin, H. Huang, B. Chen, X. Xu, J. Dai, L. Zhang, X. Yang, H. Zhai, G. Cao, and Z. Xu, preprint [arXiv:1407.3711v1](https://arxiv.org/abs/1407.3711v1).
- ³⁰A. Srivastava, A. Pal, S. Singh, C. Shekhar, H. K. Singh, V. P. S. Awana, and O. N. Srivastava, *AIP Adv.* **3**, 092113 (2013).
- ³¹T. Tomita, M. Ebata, H. Soeda, H. Takahashi, H. Fujihisa, Y. Gotoh, Y. Mizuguchi, H. Izawa, O. Miura, S. Demura, K. Deguchi, and Y. Takano, *J. Phys. Soc. Jpn.* **83**, 063704 (2014).
- ³²M. Fujioka, M. Nagao, S. J. Denholme, M. Tanaka, H. Takeya, T. Yamaguchi, and Y. Takano, *Appl. Phys. Lett.* **105**, 052601 (2014).
- ³³C. Morice, E. Artacho, S. E. Dutton, D. Molnar, H. J. Kim, and S. S. Saxena, preprint [arXiv:1312.2615v1](https://arxiv.org/abs/1312.2615v1).